Understanding selectivity in solute-solute separation: definitions, measurements, and comparability

Revised Manuscript Submitted to

Environmental Science & Technology

December 2021

Ruoyu Wang[a,$] Junwei Zhang[b,$] Chuyang Y. Tang[b] and Shihong Lin* [a,c]

[a] Department of Civil and Environmental Engineering, Vanderbilt University, Nashville, TN 37235-1831, USA

[b] Department of Civil Engineering, The University of Hong Kong, Pokfulam, Hong Kong, 999077, China

[c] Department of Chemical and Bimolecular Engineering, Vanderbilt University, Nashville, TN 37235-1831, USA

[$] R.W. and J.Z. contributed equally to this paper.

*Email: shihing.lin@vanderbilt.edu

ABSTRACT

The development of membranes capable of precise solute-solute separation is still in its burgeoning stage without a standardized protocol for evaluating selectivity. Three types of membrane processes with different driving forces, including pressure-driven filtration, concentration difference-driven diffusion, and electric field-driven ion migration, have been applied in this study to characterize solute-solute selectivity of a commercial nanofiltration membrane. Our results demonstrated that selectivity measured using different methods, or even different conditions with the same method, are generally not comparable. The cross-method incomparability is true for both apparent selectivity, defined as the ratio between concentration-normalized fluxes, and the more intrinsic selectivity, defined as the ratio between the permeabilities of solutes through the active separation layer. The difference in selectivity measured using different methods possibly stems from the fundamental differences in the driving force of ion transport, the effect of water transport, and the interaction between cations and anions. We further demonstrated the difference in selectivity measured using feed solutions containing single salt species and that containing mixed salts. A consistent protocol with standardized testing conditions to facilitate fair performance comparison between studies is proposed.

KEYWORDS

Membrane separation, solute-solute separation, resource recovery, nanofiltration, diffusion, electromigration

SYPNOSIS

Solute-solute selectivity in mixed salt separation depends on measurement method and conditions and should be interpreted and compared with caution

INTRODUCTION

Membrane separation has been applied for decades to address the global challenge of freshwater scarcity. With the development of thin-film composite polyamide (TFC-PA) membranes of high solute rejection, freshwater can now be produced efficiently using reverse osmosis (RO) or nanofiltration (NF) from wastewater and saline water.[1] Recently, precise solute separation using membranes has emerged to become one of the frontiers for membrane-based separation due to the increasing demand for selective separation,[2–5] such as nutrient recovery from wastewater,[6] water softening,[7,8] extraction of critical and strategic minerals from brines,[9–11] and industrial wastewater reuse.[12] Instead of focusing on separating all solutes from feed water, precise solute separation refers to the separation of solutes from each other with high precision, i.e., having a very high rejection for some species and a very low rejection for the others. However, precise solute separation is challenging when the solutes to be separated have similar size and charge states.

While there are other possible approaches to achieve precise solute separation (e.g., ion exchange, electrodialysis),[13,14] membrane filtration remains an attractive and the most widely studied approach due to its operational simplicity. Many studies have been devoted to design novel membranes with well-controlled structure or uniform pore size (or free volume) distribution that is indispensable for achieving more precise solute-solute separation.[15–17] General approaches taken include developing polymeric membranes (based on polyamide or alternative chemistry) with more uniform pore size distribution and using porous nanomaterials or artificial nanochannels either as fillers of nanocomposite membranes or to construct standalone active separation layers.[18] Nanomaterials that have been investigated toward this goal include carbon nanotubes,[19–21] 2D nanomaterials,[22–24] metal-organic frameworks,[25] covalent-organic frameworks,[26] and biological water channels or biomimetic artificial channels.[27,28] These membranes are often compared between each other and with commercial membranes for their performance in solute-solute separation.

The challenge with evaluating and comparing the solute-solute separation performance of novel membranes lies in the inconsistent definition and measurement methods used in different studies.[29] In general, three types of membrane processes with different driving forces have been applied to characterize solute-solute selectivity (Table 1): pressure-driven filtration (abbreviated as “filtration”, Fig. 1A), concentration difference-driven diffusion (abbreviated as “diffusion”, Fig. 1B), and electric field-driven ion migration (abbreviated as “electromigration”, Fig. 1C). Pressure-driven filtration involves applying a hydraulic pressure to drive the solution through the membrane. The membrane rejects different solutes to different extents. The performance of solute-solute separation, which is quantified using “solute selectivity”, is usually defined based on the rejection of different solutes. In concentration difference-driven diffusion, solutes transport across the tested membrane from a high-concentration feed solution to a receiving solution (typically deionized water) and the flux of solute diffusion is measured. The solute selectivity in this case is defined based on the diffusion fluxes of different solutes. Water osmosis in the opposite direction may affect solute diffusion but is typically ignored in most studies reported in literature.[30–33] In electric

field-driven ion migration, charged solutes transport through the membrane under the influence of the applied electric field. Current-voltage (I-V) curves are typically measured in a system where the membrane is positioned between two exactly same solutions. The solute selectivity in this case is defined based on membrane conductance.

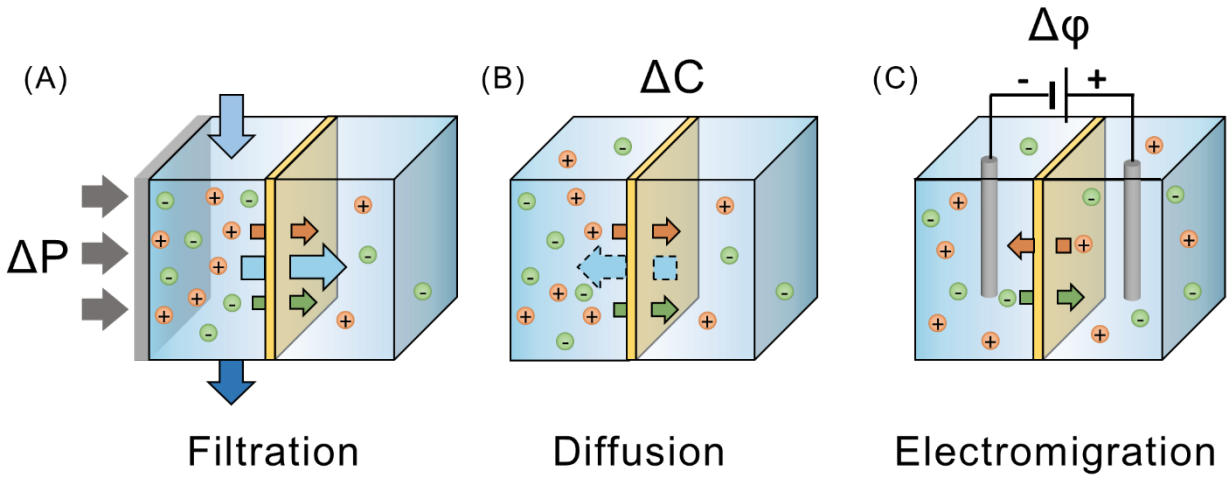

Figure 1. Schematic diagrams of (A) pressure-driven filtration process, (B) concentration difference-driven diffusion process, and (C) electro-driven migration process. Orange circles with positive sign and green circles with negative sign represent cations and anions, respectively. Grey columns represent Ag/AgCl reference electrodes. Cations and anions transport across membranes from feed to permeate in filtration and diffusion processes, while transport in the opposite direction under the electric field. Water flux in filtration is represented by the solid blue arrow. Water osmosis in diffusion process is represented as the dash blue arrow since it can be offset with the addition of sucrose in the receiving solution.

While pressure-driven filtration is practically the most relevant to the intended applications of the tested membranes, the other two methods are also commonly used especially for testing membranes that are made of novel materials. These membranes are often fabricated in a relatively small size and/or do not have sufficient mechanical strength to be tested in pressure driven filtration. The use of different evaluation methods based on fundamentally different driving forces and transport mechanisms render the comparability of the measured selectivity questionable. In fact, a summary of selected selectivity data (Table 1) suggests that the selectivity for the same separation (e.g., Li^+ and Mg^{2+} separation, which is important for lithium extraction from brine) can vary in values by more than three orders of magnitude. It is uncertain if this dramatic difference in selectivity is a result of the different membrane properties, an artifact of the different measurement methods, or likely, both. Meanwhile, even with the same measurement method, a wide range of experimental conditions (e.g., pressure, concentration, and voltage) have been used in different studies, which affect solute transport driving force and the state of membrane, and thus can be another origin of the incomparability between experimental results. Furthermore, while it is practical more relevant to measure selectivity using feed solution with mixed salts, most studies in literature evaluated selectivity using results from experiments performed with feed solutions

containing a single salt species. It is thus also uncertain if selectivity measured using single-salt and mixed-salt feed solutions are comparable.

Table 1. Examples of studies from literature using different methods for selectivity evaluation

Methods	Single /Mixture	Conditions	Membranes	Solute pairs	Selectivity
Filtration	Single	1000 ppm, 10 bar	Conjugated microporous polymer membrane[30]	K^+, Na^+, Li^+, Ca^{2+}, Mg^{2+} vs Al^{3+}, $Fe(CN)_6^{3-}$	6~10
		10 mM, 3 bar	Nanocavity-contained TFC-NF membrane[34]	Cl^- vs SO_4^{2-}	5~35
		500 ppm, 5 bar	Zwitterionic TFC-NF membrane[35]	Cl^- vs SO_4^{2-}	12~16
	Mixture	1 to 5 mM, 3.45 bar	Polyelectrolyte multilayer NF membrane[8]	Na^+ vs Ca^{2+}, Mg^{2+}	1~40
		2000 ppm (1:20), 8 bar	PEI-TMC NF membrane[36]	Li^+ vs Mg^{2+}	~16
		2000 ppm (1:23), 5 bar	Cu-MPD membrane[11]	Li^+ vs Mg^{2+}	~8
Diffusion	Single	10 mM, 24 hours	Conjugated microporous polymer membrane[30]	K^+, Na^+, Li^+, Ca^{2+}, Mg^{2+} vs Al^{3+}, $Fe(CN)_6^{3-}$	100~1000
		1 M, 5 days	GO membrane[31]	K^+, Na^+, Li^+ vs Ca^{2+}, Mg^{2+}	>100
		200 mM, 4 hours	2D $Ti_3C_2T_x$ MXene membrane[32]	K^+, Na^+, Li^+ vs Ni^{2+}, Ca^{2+}, Mg^{2+}	~5
	Mixture	1 M, 30 days	PVC/MOF hybrid membrane[33]	Li^+ vs Mg^{2+}	~5
Electro-migration	Single	10 mM, -0.5 to 0.5 V	Conjugated microporous polymer membrane[30]	K^+ vs Na^+, Li^+, Ca^{2+}, Mg^{2+}, Al^{3+}, $Fe(CN)_6^{3-}$	1.1~20
		0.05 to 500 mM, -0.4 to 0.4 V	PSS threaded MOF membrane[37]	Li^+ vs K^+, Na^+, Mg^{2+}	80~10^4
		1 to 1000 mM, -10 to 10 V	GeV irradiated PET film[38]	K^+, Na^+, Li^+, Cs^+ vs Mg^{2+}, Ca^{2+}, Ba^{2+}	10~10^5

In this study, we evaluate and compare the selectivity between different ions with a commercial NF membrane using three different approaches: filtration, diffusion, and electromigration. We perform experiments using these three methods with single-salt solutions of

NaCl, Na_2SO_4 and $MgCl_2$ at different concentrations to evaluate the monovalent/divalent selectivity for anions and cations. For filtration experiments, the impact of operating pressure is also evaluated. The apparent selectivity and selectivity based on more intrinsic membrane properties are both compared between the three different methods. In addition, we also evaluate selectivity measured with single-salt and mixed-salt feed solutions using both filtration and diffusion experiments.

MATERIALS AND METHODS

Materials and experimental setups

A commercial polyamide NF membrane, NFX (Synder, TFC-PA, MWCO=150-300 Da), was used in this study for all experiments. Three common salts, NaCl, Na_2SO_4 and $MgCl_2$, were used to evaluate membrane solute-solute selectivity. Three types of experiments that have been used in literature for measuring selectivity were performed, including pressure-driven filtration, concentration difference-driven diffusion, and electro-driven migration. For pressure-driven filtration, a crossflow filtration system with three parallel commercial filtration cells (Sterlitech, CF042) was used in NF experiments. The effective membrane area of each cell was 42 cm^2. For concentration difference-driven diffusion, a U-shaped diffusion cell (Pasco, ME-6940) was used in diffusion experiments. The U-shaped cell was composed of two columns separated by a semi-permeable membrane. The effective membrane area was 2.84 cm^2. For electro-driven migration, a Side-Bi-Side electrochemical cell (PermeGear) was used in linear sweep voltammetry (i.e., I-V curve measurements). The cell comprised two 7 mL-volume chambers separated by a semi-permeable membrane. The effective membrane area was 0.2 cm^2. An Ag/AgCl reference electrode (CH Instruments, CHI111) was inserted in each chamber. A potentiostat (Biologic, SP-200) was used to apply voltage across the electrochemical cell and record current. In all experiments, salt solutions were prepared with deionized water. The equilibrium solution pH (unadjusted) was in the range of 6~7 and did not show any observable change throughout the filtration experiments.

Pressure-driven nanofiltration ("filtration")

Pressure-driven NF experiments were carried out in a crossflow filtration system at a crossflow velocity of ~20 cm s^{-1} under room temperature (25 ˚C). The single salt rejections of the NFX membrane were determined using a single salt feed solution containing either NaCl, or Na_2SO_4 or $MgCl_2$ at a series of concentration of 5, 15, 25, 50 and 100 mM, respectively. The NF membranes were pre-compacted for 2 hours to reach a steady state before tuning the operating pressure to achieve a designated permeate flux (i.e., 25, 35, 50 and 70 L m^{-2} h^{-1}) for each individual membrane coupon. Permeate conductivity was then measured and converted to salt concentration based on a calibration curve relating the two parameters. The permeate salt concentration was used to calculate the salt rejection. New membrane samples were used for different salts and different

concentrations, but the same membranes were used when varying permeate flux. All data points were obtained based on results from three replicates.

To evaluate the difference between selectivity measured with feed solutions containing a single salt species and that measured with feed solutions containing a mixture, NF experiments were also performed with feed solutions containing a mixture of NaCl and $MgCl_2$ at different concentrations. The molar concentration ratio of the two salts was 1:1 with each salt concentration to be 25, 50 and 100 mM. The operating pressure was tuned to achieve a permeate flux of 30 L m^{-2} h^{-1}. The concentrations of Na^+ and Mg^{2+} in the permeate were measured by inductively coupled plasma optical emission spectrometry (ICP-OES) for rejection calculation.

The permeate flux, J_w, of the NF experiments was determined using the following equation:

$$J_w = \frac{\Delta V}{A_F \Delta t} \tag{1}$$

where ΔV is the permeate volume produced in the period of Δt and A_F is the effective filtration area of the membrane coupon. The observed salt rejection, R, was defined as:

$$R = 1 - \frac{C_p}{C_f} \tag{2}$$

where C_p and C_f are molar concentrations of target solute in the permeate and feed solution, respectively. The solute-solute selectivity in pressure-driven filtration, S_F, is typically defined based on solute rejections using the following expression:[8]

$$S_F = \frac{1 - R_a}{1 - R_b} \tag{3}$$

where subscripts a and b represent solutes a and b, respectively. Conventionally, the more permeable solute is assigned to the numerator and the less permeable solute to the denominator, so that S_F is larger than unity and a larger S_F represents better solute-solute selectivity. When evaluating the selectivity between monovalent and divalent ions, such a convention means that the rejection of monovalent ions is assigned to the numerator and that of divalent ions to the denominator since divalent ions are usually better rejected than monovalent ions (if the membranes and ions are of similar charge). To better understand the physical meaning of the rejection-based selectivity, Eq. (3) can be rewritten in an equivalent form by substituting the rejection terms with Eq. (2) as:

$$S_F = \frac{C_{p,a}/C_{p,b}}{C_{f,a}/C_{f,b}} = \frac{J_a/C_{f,a}}{J_b/C_{f,b}} \tag{4}$$

where J_a and J_b represent steady-state solute flux of a and b, respectively. The first part of Eq. (4) suggests that the selectivity can be interpreted as the ratio between the abundance of species a (relative to b) in permeate and that in the feed solution. The second part of Eq. (4) utilizes the

relationship between solute flux (J_s) and permeate flux (J_w) at steady state, $J_s = J_w C_p$. Selectivity based on this definition can be interpreted as the ratio of the concentration-normalized flux between the two solutes. According to Eqs. (3-4), a highly precise solute separation results from almost no rejection to the more permeable solute but nearly perfect rejection to the less permeable solute.

Concentration difference-driven diffusion ("diffusion")

Concentration-driven diffusion experiments were conducted using a U-shaped diffusion cell. The NFX membrane was clamped in the middle the cell to separate the feed solution and permeate, with the polyamide surface facing the feed solution. For experiments with single-salt feed solution, the feed side of the diffusion cell was filled with a 20 mL solution of NaCl, Na_2SO_4, or $MgCl_2$ at a range of concentrations including 5, 25, 50, 100, 250 and 500 mM. The permeate side was filled with 20 mL of either pure water or sucrose solution. Sucrose (MW=342 Da) was used to offset the osmotic pressure difference to minimize the effect of osmosis. The concentration of the sucrose solution was determined based on the osmotic pressure of the feed solution as estimated using the van't Hoff relation:

$$\Delta\pi = \nu C R_g T \tag{5}$$

where $\Delta\pi$ is osmotic pressure, ν is van 't Hoff factor (one for sucrose), C is solute molar concentration, R_g is ideal gas constant and T is solution temperature. Both feed and permeate solutions were continuously stirred with stir bars to minimize concentration polarization (CP) near the membrane-solution interfaces. Each diffusion experiment lasted for one hour during which the permeate conductivity was measured and later converted to salt concentration based on the calibration curve relating the two parameters.

To evaluate the selectivity measured with mixed salt feed solutions, diffusion experiments were performed with NaCl and $MgCl_2$ mixture feed solutions at different concentrations. The molar concentration ratio of two salts in the feed solution was 1:1, with each salt concentration set to be 25, 50 or 100 mM. The receiving solution was either pure water, in which case the osmotic flow was not corrected, or sucrose solution to offset the osmosis. The Na^+ and Mg^{2+} concentrations in the receiving solutions were measured using ICP-OES to determine the diffusion fluxes. New membrane samples were used for different salts and different concentrations. All data points were obtained based on results from three replicates.

The average solute diffusion flux, J_D, in diffusion experiments can be estimated from mass accumulation rate of target solute in the permeate:

$$J_D = \frac{V C_p}{A_D \Delta t} \tag{6}$$

where V is the permeate solution volume, C_p is the solute molar concentration in the permeate after a period Δt, and A_D is the effective membrane area of the diffusion cell. The solute-solute selectivity in concentration-driven diffusion, S_D, is typically defined based on the diffusion flux as:[31]

$$S_D = \frac{J_{D,a}/C_{f,a}}{J_{D,b}/C_{f,b}} \quad (7)$$

where C_f is molar concentration of target solute in the feed, and subscripts a and b represent solute a and b, respectively. Like Eq. (4), Eq. (7) defines the selectivity as the ratio of the concentration-normalized flux between the two solutes.

Electric field-driven ion migration ("electromigration")

Electro-driven migration experiments were conducted using a Side-Bi-Side electrochemical cell. The NFX membrane was clamped between the anode and cathode chambers. Both chambers were filled with 7 mL of NaCl, Na_2SO_4 or $MgCl_2$ single salt solutions of same concentration (i.e., 5, 25, 50, 100, 250 and 500 mM). Linear sweep voltammetry (LSV) was performed over the voltage range of -50 mV to 50 mV at a scan rate of 2 mV s^{-1}. The I-V curves in this range showed linear relationship and were fitted to obtain the overall conductance of solution and membrane, G_t. I-V curves under the same conditions were also measured without membranes to obtain conductance of solution, G_s. New membrane samples were used for different salts and different concentrations. All data points were obtained based on results from three replicates. Assuming solution and membrane as an equivalent circuit of resistance in series, the conductance of membrane, G_m, can be then evaluated from:

$$\frac{1}{G_t} = \frac{1}{G_s} + \frac{1}{G_m} \quad (8)$$

According to Eq. (8), G_m can be approximated by G_t if and only if $G_s \gg G_m$. We note that this approximation has been frequently used when evaluating selectivity with electro-driven processes in literature but is nonetheless not always valid. The membrane conductance for ion transport in an electro-driven process can be described as:[39]

$$G_m = \frac{A_{EM}F}{\Delta\varphi}\sum_i J_i|z_i| \quad (9)$$

where A_{EM} is the effective membrane area of the electrochemical cell, F is the Faraday constant, $\Delta\varphi$ is the voltage across the membrane, J_i and z_i are the flux and valence of ion species i, respectively. By rearranging Eq. (9), the ion flux of species i can be expressed as:

$$J_i = \frac{G_m \Delta\varphi T_i}{A_{EM}F|z_i|} \quad (10)$$

where T_i is the transport number of ionic species i, which represents the fraction of overall current carried by this species (vs. other ionic species)[40]:

$$T_i = \frac{J_i|z_i|}{\sum_k J_k|z_k|} \tag{11}$$

Analogous to the selectivity definitions in pressure-driven filtration and concentration difference-driven diffusion, the solute-solute selectivity in electro-driven migration, S_{EM}, can be defined as the ratio of the concentration-normalized flux between the two solutes:

$$S_{EM} = \frac{J_a/C_{f,a}}{J_b/C_{f,b}} = \left(\frac{G_{m,a}/C_{f,a}}{G_{m,b}/C_{f,b}}\right)\left(\frac{T_a/|z_a|}{T_b/|z_b|}\right) = \left(\frac{G_{m,a}/C_{f,a}}{G_{m,b}/C_{f,b}}\right)\left(\frac{t_a}{t_b}\right) \tag{12}$$

We note that a ratio of absolute valence-normalized transport number (i.e., also known as transference number, $t_i = T_i/|z_i|$) appears in the conductance-based selectivity when substituting ionic flux with Eq. (10). This ratio in the second parentheses is usually omitted in literature, which is only valid under the following conditions: (1) the ionic species of interest have the same transference number (i.e., $t_a = t_b$); (2) the ionic species of interest (in single salt experiments) have the same valence and carry all the current and thus transport number is unity. The first assumption has no theoretical basis whereas the second assumption is acceptable only when evaluating selectivity between ionic species of same valence and the membrane has a high charge density (e.g., ion exchange membranes). In this study, we evaluated these assumptions for NFX membrane by determining the transport numbers of each ionic species.

To determine the transport numbers of cation and anion for each single salt, the concentration was maintained constant in the high-concentration chamber (i.e. C_h = 100 mM), while the concentration in the low-concentration chamber, C_l, gradually varies from 5 to 25, 50 and 100 mM to obtain concentration ratios (between the two chambers) of 20:1, 4:1, 2:1 and 1:1, respectively. At each concentration ratio, LSV measurement was performed and the membrane potential, $\Delta\varphi_m$, was determined as the intersect between the I-V curve and the voltage axis. The transport number was then calculated using the following equation:[39]

$$\Delta\varphi_m = (t_+ - t_-)\frac{RT}{F} ln\left(\frac{C_h}{C_l}\right) \tag{13}$$

where subscripts + and − represent cation and anion, respectively.

RESULTS AND DISCUSSION

Selectivity depends on measurement conditions

Filtration Feed concentration and permeate flux both affect salt rejections by NF membranes.[41] NFX membrane showed 95%~99% rejections to $MgCl_2$ and Na_2SO_4 in a wide range of feed concentration and permeate flux, while NaCl rejection varied from 30% to 65% (Fig. S1). To evaluate the effect of feed concentration on solute-solute selectivity, we focused on rejections of

single salt in the concentration range of 5 to 100 mM under the same permeate flux (i.e., 50 L^{-1} m^{-2} h^{-1}). Selectivity of mono-/divalent anions (i.e., Cl^-/SO_4^{2-}) and cations (i.e., Na^+/Mg^{2+}) defined based on Eq. (3) exhibited similar trends of variation with increasing feed concentration (Fig. 2B). As the solute concentration increased, both Na^+/Mg^{2+} and Cl^-/SO_4^{2-} selectivity improved because NaCl rejection decreased from 60% to 36%, while the rejections of $MgCl_2$ and Na_2SO_4 remained around 97% (Fig. 2A).

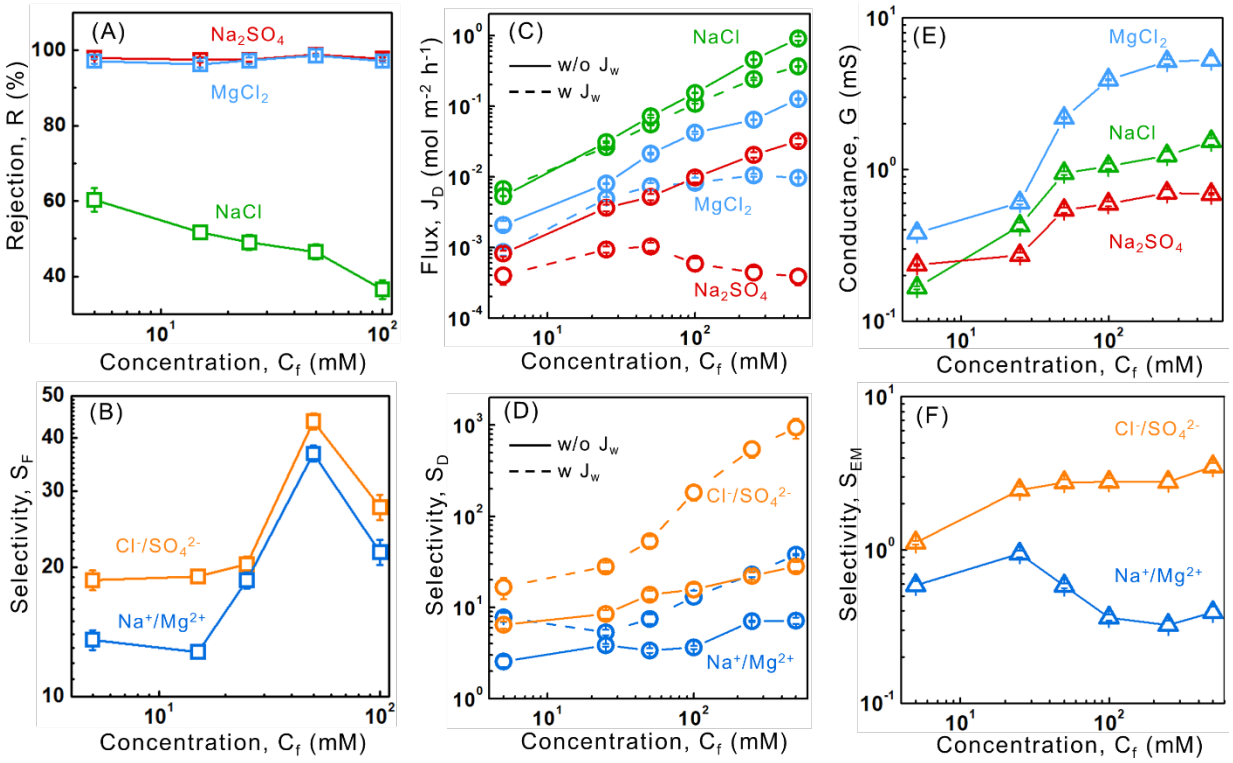

Figure 2. (A) Salt rejection and (B) selectivity defined on rejection as a function of feed concentration. Filtration pressure was tuned to maintain a permeate flux of 50 L m^{-2} h^{-1}. (C) Diffusion flux and (D) selectivity defined on diffusion flux as a function of feed concentration. Diffusion flux was determined from salt mass accumulation rate in the permeate solution. Sucrose was added in the receiving solution to offset water osmosis (solid curves). (E) Membrane conductance from I-V curve results and (F) selectivity defined on conductance as a function of solution concentration. I-V curves were obtained via linear sweep voltammetry characterized within -50 to 50 mV at a scan rate of 2 mV/s. We note that axis has different scale in each panel.

The reduced rejection of NaCl at a higher feed concentration can be attributed to the stronger charge screening effect at a high ionic strength, which reduced the electrostatic (Donnan) exclusion to NaCl.[42,43] Although the same effect also applies to $MgCl_2$ and Na_2SO_4, their rejections were largely unaffected as their transport was more constrained due to the presence of large divalent ions (Mg^{2+} and SO_4^{2-}) with stronger steric hindrance,[44] lower diffusivity,[45,46] and stronger hydration energy.[47] Therefore, the unaffected rejections of $MgCl_2$ and Na_2SO_4, combined with the compromised rejection of NaCl at a higher feed concentration resulted in a generally increasing Na^+/Mg^{2+} and Cl^-/SO_4^{2-} selectivity as the feed concentration increased.

The only exception to this trend in the collected data is the reduced Na^+/Mg^{2+} and Cl^-/SO_4^{2-} selectivity when the feed concentration increased from 50 to 100 mM. However, the rejection data in Fig. 2A show no significant deviation from the trend for the rejection of all salts at any specific concentration. The very high selectivity observed at 50 mM is caused by the slightly higher rejection of $MgCl_2$ and Na_2SO_4 as compared to the already-very-high rejection of the same salts at 100 mM. Whether this difference can be explained or is simply caused by measurement error, its magnitude is very small (98.5% vs. 97.1% for $MgCl_2$, and 98.8% vs. 97.7% Na_2SO_4), particularly compared to the much more salient difference of rejection for NaCl measured at these two concentrations (46.5% vs. 36.5%). However, this small difference of the rejection for the less permeable salt has a very large influence on selectivity via affecting the very small denominator in Eq. (3). In other words, the rejections of the salts in the numerator and denominator have disproportionate impacts on the selectivity. The selectivity is more sensitive to the rejection of the less permeable salt (in the denominator), especially when its rejection approaches 100%. We note that the appropriateness of a sensitivity definition may depend on the specific application scenarios (e.g., removal of the less permeable solute vs. recovery of the more permeable solute) and is worthy of further discussion beyond this study.

The effect of permeate flux on selectivity in pressure-driven filtration was also evaluated. It is well known, as the dilution effect, that increasing the permeate flux typically enhances salt rejection unless in the case when ion transport mechanism is dominated by advection (which is usually considered not the case for nanofiltration).[48,49] In our experiments, the rejection of NaCl increased by ~10% when the permeate flux increased from 35 to 70 L m^{-2} h^{-1}, regardless of the feed concentration (Fig. S1A). The rejections of $MgCl_2$ and Na_2SO_4 also increased but to a much smaller extent (Fig. S1B, C), because the rejections, even with the lowest permeate flux, were higher than 95% to start with. Even though the rejection of NaCl was considerably more sensitive than $MgCl_2$ and Na_2SO_4 to the change of flux, the selectivity of Na^+/Mg^{2+} or Cl^-/SO_4^{2-} remained roughly unchanged (Fig. 3), which can again be explained by the disproportionate impacts of variation in rejection for species in the numerator vs. that in the denominator according to Eq. (3). In short, while increasing the permeate flux improved the rejection of NaCl, it has a weak impact on the Na^+/Mg^{2+} and Cl^-/SO_4^{2-} selectivity.

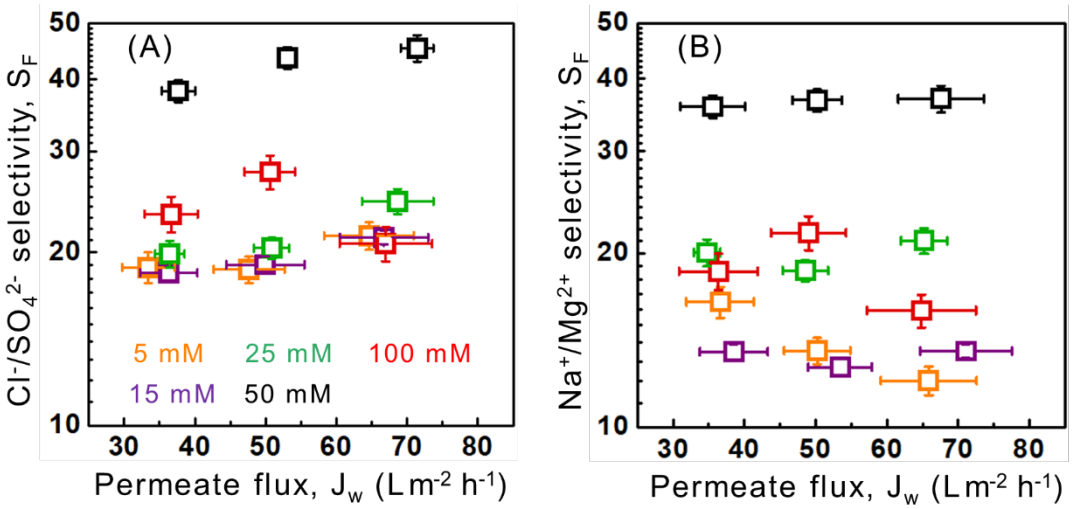

Figure 3. (A) Cl^-/SO_4^{2-} selectivity and (B) Na^+/Mg^{2+} selectivity defined on rejection as a function of permeate flux under different feed concentrations.

Diffusion During the one-hour diffusion experiments, permeate concentration increased almost linearly over time except for the first 5~10 minutes when the salt ions have not permeated through the membrane (Fig. S2). As the salt concentration in the feed solution was much higher than that in the receiving solution, the concentration difference across the membrane can be regarded as approximately constant throughout the experiment and the diffusion can be considered as steady state. With sucrose in the receiving solution to balance osmotic pressure difference (solid curves in Fig. 2C and 2D), diffusion flux increased linearly with feed concentration for all three salts, because concentration difference (or chemical potential difference) was the driving force for diffusion. Both cation and anion selectivity defined based on diffusion flux increased monotonously with feed concentration and anion selectivity was higher than cation (Fig. 2D).

When pure water was used as the receiving solution (without sucrose, dash curves in Fig. 2C and 2D), its volume decreased over time due to osmosis. As a result, all salt fluxes decreased as compared to those measured with a sucrose-containing receiving solution, particularly at a higher feed concentration and for salts with a higher van't Hoff factor. For example, with a 500 mM feed concentration, the Na_2SO_4 diffusion flux measured with osmosis was about two orders of magnitude smaller than that measured without osmosis. As the effect of osmosis is substantially less significant with NaCl than with $MgCl_2$ or Na_2SO_4 (at the same molar concentration), both cation and anion selectivity measured in the presence of osmosis (i.e., without offset) were higher than selectivity measured with osmosis offset by sucrose (Fig. 2D). At high feed concentrations, the anion selectivity with and without osmosis offset differed by two orders of magnitude.

The salt flux decline caused by osmosis is attributable to the interference between water and ions transport in the opposite directions across the membrane. Since $MgCl_2$ and Na_2SO_4 solutions have higher osmotic pressures than NaCl at a same feed concentration, larger osmosis fluxes were generated to counter the ion transport. In addition, the ion size and diffusivity also

contribute to the difference in flux decline between salts. However, it is not completely clear if the negative impact of a water flux in the opposite direction (of the salt flux) on the salt flux was exerted through both the support layer (i.e., internal concentration polarization, ICP) and the active layer, or just one of them. Regardless of the distribution between different mechanisms, our results suggest unequivocally that the osmosis effect is salient and cannot be ignored. Unfortunately, this osmosis effect has been often ignored in previous studies using concentration-driven diffusion experiments even with higher feed concentrations (e.g., 1~2 M) and very long diffusion time (e.g., hours or days).[30–33] Although using a diffusion cell with a small membrane area may reduce the effect of dilution (of the feed solution) and concentration (of the receiving solution) due to solution volume change caused by osmosis, the effect of osmosis in reducing salt flux can still be significant and is independent of membrane area.

Electromigration Membrane conductance with single salt feed solutions of different concentrations was determined from I-V curves measured using LSV with and without a membrane (Fig. S3). As polyamide NF membrane is nonconductive, the current is all carried by transport of ions across the membrane. Membrane conductance in all salt solutions increased with solution concentration (Fig. 2E). In general, the conductance at the same concentration follows the order of $MgCl_2$ > NaCl > Na_2SO_4, because transport through a negatively charged NF membrane is more favorable for divalent cations (Mg^{2+}) than for monovalent cations (Na^+) and less favorable for divalent anions (SO_4^{2-}) than for monovalent anions (Cl^-).

Anion selectivity defined based on conductance slightly increased with concentration while cation selectivity did not follow a monotonic trend (Fig. 2F). We note that cation and anion transport are decoupled in electro-driven process, while they are paired to maintain electro-neutrality in the other two methods.[39] In this regard, cation or anion selectivity characterized using the electromigration method is more consistent with its name. We also note that, as mentioned in Section 2, the conductance-based selectivity usually omits the transport number ratio in Eq. (12) by assuming that the current is all carried by the ionic species of interest. In this study, the transport numbers of cation and anion for the NFX membrane were evaluated by the membrane potential method described in Section 2 (Fig. S4). $T_{Na^+}/T_{Mg^{2+}}$ and $T_{Cl^-}/T_{SO_4^{2-}}$ were estimated to be 0.67 and 0.79, respectively, which should not be omitted.

Selectivity is not comparable between methods

For a fair comparison of novel membranes from literature, we expect the solute-solute selectivity of the same membrane characterized by different methods to be same or at least similar. This is, however, not the case for selectivity defined based on the ratios of feed concentration-normalized solute fluxes. While different methods show qualitatively similar trends regarding the effect of concentration and the comparison between anion and cation selectivity, they do not yield quantitatively comparable results (Fig. 2B, D and F). For example, anion selectivity varied between 20~50 within the concentration range of 5 to 100 mM when defined based on rejection in

pressurized filtration. It was around 10 when defined based on diffusion flux without osmosis and varied from 10 to over 100 in the presence of osmosis. For electromigration, the anion selectivity of the same concentration range was lower than 10.

One possible explanation for the incomparability of selectivity measured using different methods is that feed concentration-normalized solute flux does not capture the intrinsic permeability of the solute through the active layer of the membrane. In diffusion-based selectivity (Eq. (7)), the concentration difference across the membrane is the driving force. When ignoring concentration polarization (CP), the driving force is practically equal to the feed concentration (as the concentration of the receiving solution is essentially zero). In this case, the feed concentration-normalized diffusion flux is the solute permeability. Therefore, the physical meaning of diffusion-based selectivity is the solute permeability ratio. Although the other two types of selectivity (based on filtration and electromigration) were also defined in a similar form as the ratio between feed concentration-normalized solute fluxes (Eqs. (4 and 12)), the differences in measured selectivity values arise from the fact that the different measurements characterize different transport phenomena in terms of driving force, presence of water transport, and the state of coupling between cation and anion transport. In the following discussion, we will show that solute permeabilities across membrane, and thus the ratio between permeabilities of different solutes, are also dependent on the measurement method and thus cannot be considered as an intrinsic membrane property.

Filtration Solute transport through polyamide membranes in pressurized filtration process has been widely studied for decades. The description of solute transport through polyamide membranes was initially described by phenomenological equations based on irreversible thermodynamics, and later simplified to the solution-diffusion (S-D) model. S-D model, typically applied to "dense membranes" used in RO, gas separation, or pervaporation, assumes that both water and solutes first dissolve (or partition) into the membrane and then diffuse through the membrane matrix.[50] Within the S-D framework, solute permeability, B, is defined as:

$$B = \frac{KD_m}{d_m} = \frac{J_s}{C_f - C_p} \tag{14}$$

where K, D_m and d_m are partition coefficient, diffusion coefficient in the membrane active layer, and membrane active layer thickness. The solute permeability relates solute flux, J_s, to the solute concentration difference, $C_f - C_p$. Water transport and solute transport are assumed to be independent in S-D model. The applicability of the S-D model in describing transport in NF is questionable as NF membranes have a 'looser' polymer matrix (or larger pore size) with which advection may have a more significant contribution to solute flux. Nonetheless, here we still adopt the phenomenological S-D model framework to examine solute-solute selectivity in pressure-driven filtration while being aware of the caveat that the solute permeability may be dependent on experimental conditions instead of being an invariant membrane property.[41]

By describing concentration polarization (CP) with thin film theory, the *intrinsic* solute permeability of a pressure-driven filtration process, B_F, can be determined with permeate flux and solute rejection as:[51]

$$B_F = J_w \left(\frac{1}{R} - 1\right) e^{-\frac{J_w}{k}} \tag{15}$$

where k is mass transfer coefficient of solute (k = 70.4, 72.2, 67.2 L m^{-2} h^{-1} for NaCl, Na_2SO_4 and $MgCl_2$) and was pre-determined by the flux method proposed by Tang et al.[51] With Eq. (15), we found that $MgCl_2$ and Na_2SO_4 had similar intrinsic permeability and were over an order of magnitude lower than that of NaCl (Fig. 4A), which was consistent with the observed rejection difference between these salts. The solute-solute selectivity defined based on the ratio of intrinsic permeabilities measured using a filtration process, S_F^B, was then determined as:

$$S_F^B = \frac{B_{F,a}}{B_{F,b}} = S_F \frac{R_b}{R_a} e^{\frac{J_w}{k_b} - \frac{J_w}{k_a}} \tag{16}$$

where S_F^B relates to the apparent (or measured) selectivity, S_F, by a correction factor being the product of the rejection ratio and an exponential term accounting for the difference in CP between the two solutes.

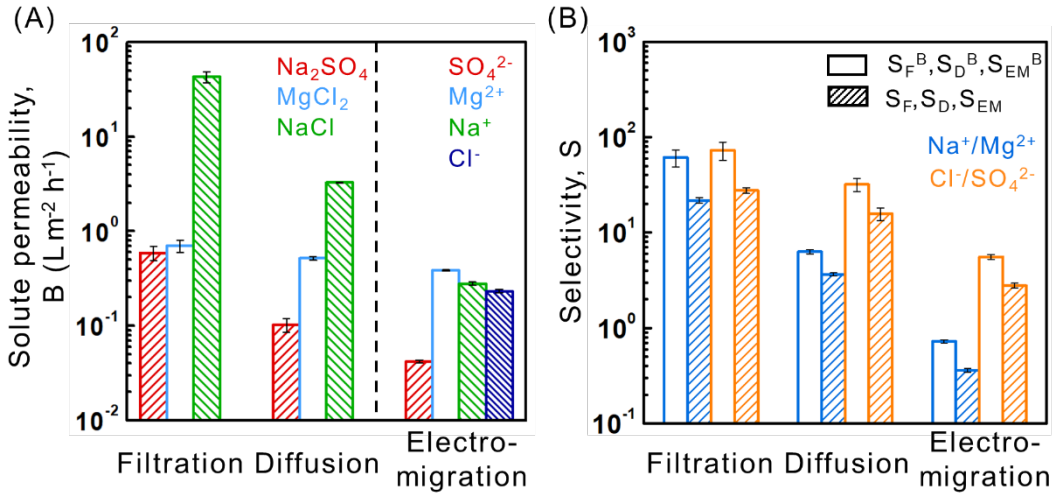

Figure 4. (A) Solute permeability and (B) Na^+/Mg^{2+} selectivity and Cl^-/SO_4^{2-} selectivity of different definitions under 100 mM solution concentration. Diffusion data was from experiments without osmosis.

Diffusion In concentration difference-driven diffusion with osmosis offset, by applying the model framework of solution-diffusion and considering CP, the solute diffusion flux can be expressed as:[52]

$$J_D = k(C_f - C_p) = \left(\frac{1}{k_f} + \frac{1}{k_p} + \frac{s}{D} + \frac{1}{B_D}\right)^{-1} (C_f - C_p) \approx \left(\frac{s}{D} + \frac{1}{B_D}\right)^{-1} C_f \tag{17}$$

where k is overall apparent solute permeability, k_f and k_p are mass transfer coefficients in feed and permeate boundary layers accounting for external CP (ECP), s and D are structural parameter of the porous support layer of NF membrane and solute diffusion coefficient in the solution. s/D accounts for CP effect inside the support layer, i.e., the internal concentration polarization (ICP). B_D is solute permeability for diffusion across the polyamide active layer. If we assume external CP is negligible compared to ICP due to continuous stirring of feed and permeate during experiments, the two mass transfer coefficients can be dropped, resulting in a simplified version of the expression (third part of Eq. (17)). We also assume s to be 2000 μm, a reasonable value for the porous support of TFC-PA NF membranes. With these assumptions, the solute permeability across the active layer, B_D, can be estimated using the diffusion flux, J_D. Our experimental results suggest that NaCl has the highest permeability, followed by $MgCl_2$ and lastly Na_2SO_4 (Fig. 4A). The difference in permeability was around an order of magnitude.

Once B_D can be evaluated, the solute-solute selectivity defined based on permeability ratio in a diffusion process, S_D^B, can be estimated using Eq. (18):

$$S_D^B = \frac{B_{D,a}}{B_{D,b}} = \frac{\left(\left(\frac{J_{D,a}}{C_{f,a}}\right)^{-1} - \frac{s}{D_a}\right)^{-1}}{\left(\left(\frac{J_{D,b}}{C_{f,b}}\right)^{-1} - \frac{s}{D_b}\right)^{-1}} \tag{18}$$

Comparing with Eq. (7) which yields the apparent selectivity in the presence of the CP, Eq. (18) characterizes the intrinsic selectivity of the active layer. Our analysis shows that S_D^B is larger than the apparent selectivity, S_D, because of ICP (Fig. 4B).

Electromigration The ionic flux in electro-driven membrane process can be described by the Nernst-Planck equation as:

$$J_i = |z_i| D_{m,i} K_i C_i \frac{F}{RT} \frac{\Delta\varphi}{d_m} \tag{19}$$

By grouping diffusion and partition coefficients and membrane thickness, a solute permeability with the same form as those in filtration and diffusion processes can be defined by combining Eq. (10) and Eq. (19):

$$B_{EM,i} = \frac{RT}{|z_i|^2 F^2 A_G C_i} G_{m,i} T_i \tag{20}$$

Since NFX is negatively charged (but not as strongly charged as a cation exchange membrane), the permeability of SO_4^{2-} was the lowest and the permeability of Mg^{2+} was the highest. The permeabilities of Na^+ and Cl^- were between that of SO_4^{2-} and Mg^{2+} but much closer to the latter (Fig. 4A). The intrinsic solute-solute selectivity defined based on permeability ratio in the electro-driven process, S_{EM}^B, is determined as:

$$S_{EM}^{B} = \frac{B_{EM,a}}{B_{EM,b}} = S_{EM}\frac{|z_b|}{|z_a|} \quad (21)$$

where S_{EM}^{B} was related to S_{EM} by a factor of the valence ratio. The valence ratio, $|z_b|/|z_a|$, equals 2 when evaluating mono-/divalent ion selectivity. Therefore, S_{EM}^{B} is twice as S_{EM} (Fig. 4B).

Cross-method comparison To compare the solute permeability determined from different methods and the permeability-based selectivity between methods, we focused on one feed concentration (i.e., 100 mM) in the following discussion, whereas results obtained with other concentrations are also presented in the supporting information (Fig. S5). If the theoretical framework of solution-diffusion were applicable for NFX membrane, the intrinsic solute permeability determined from filtration should be the same as that from diffusion process. However, for NaCl, B_D was only 7.6% of B_F while the percentages were 17.3% and 74% for Na_2SO_4 and $MgCl_2$ (Fig. 4A). The lower permeability values from diffusion may be attributed to an overestimation of effective driving force if CP effect (both external and internal) is not fully considered. For filtration, ECP at feed side has been accounted by film theory and there is no ICP in the support layer at steady state. For diffusion, the minimization of ECP strongly depends on the stirring speed (i.e., degree of hydrodynamic mixing) which can be limited by the diffusion cell geometry. Meanwhile, ICP in the support layer can significantly reduce the effective driving force for diffusion even when osmosis is offset. Assume that the solute permeability were indeed the same in filtration and diffusion, we can then estimate the structural parameters required for the correction based on Eq. (17). The estimated structural parameters are 3,630 μm for NaCl, 4,835 μm for $MgCl_2$, and 48,900 μm for Na_2SO_4 with a feed concentration of 100 mM and vary with a different feed concentration. However, the structural parameter should in theory depend only on the geometry of the support layer but not on the salt properties and concentration and should therefore have a single value regardless of the feed solution. We thus conclude that the difference between permeabilities measured using diffusion and filtration cannot be reconciled simply by a more accurate structural parameter, and that there exist other mechanisms that contribute to the lower permeability values in diffusion.

Another major difference between the filtration and diffusion is the presence of water flux in filtration, which suggests that advection may have a non-negligible contribution to solute transport through the membrane matrix and challenges the assumption of the S–D model framework. Furthermore, advective flux can also affect ion electromigration (not as a measurement method by as a mechanism of ion transport in the pore-flow model) via inducing transmembrane potential.[53] The coupled effect of water flux on solute permeability is also supported by the observed solute flux decline when osmosis was not offset in the diffusion experiments (Fig. 2C). Solute permeability increases when there is water transport in the same direction and decreases if water flows in the opposite direction. Additionally, the difference of B_D/B_F between different salts shows the advection contribution to overall solute permeability depends on solute properties, which is corroborated by the Donnan Steric Pore-flow model that describes the advective

contribution of solute transport using a hindrance coefficient that is a function of the ratio between solute size and membrane pore size.[41]

Lastly, solute permeability determined from electromigration was smaller than that from diffusion and filtration (Fig. 4A), possibly due to the decoupled ion transport in the electro-driven process where ion-ion friction may play a role.[54] This decoupling may cause the partition and diffusion coefficients to be different from that for transport with paired salts. The solute-solute selectivity for electromigration through NFX membrane is also lower than that in filtration and diffusion (Fig. 4B). The incomparability of solute-solute selectivity measured using different methods is further confirmed by a separate series of data measured using a completely different membrane as reported in a very recent study.[30] Specifically, the cation permeability measured using filtration, diffusion, and electromigration exhibit difference by orders of magnitude (Fig. S6A). Both the apparent and intrinsic selectivity for different cation pairs is incomparable between different methods to various degrees (Fig. S6B). Understanding these differences measured using different methods likely require a more comprehensive ion transport model framework based on Nernst-Planck and Maxwell-Stefan equations to account for advection, diffusion, electromigration and frictions between all components (e.g., solute-solute, solute-water, solute-membrane), in addition to proper consideration of concentration polarization. Under such a framework, solute permeability would become an oversimplified phenomenological variable with little mechanistic significance and cannot serve as the basis for defining selectivity. In other words, we cannot make apparent selectivity "more intrinsic" by using solute permeability which is by itself not an intrinsic property.

Single-salt and mixed-salt feed solutions yield different selectivity

In previous discussion, solute-solute selectivity was measured with two single-salt solutions rather than with a feed solution of mixed salts. While solute-solute selectivity is only practically meaningful for separating a salt mixture, the reports of solute-solute selectivity measured using single-salt solutions are very common in literature, particularly for diffusion and electromigration. In fact, all electromigration experiments based on conductance measurements only used single-salt solution because the transport number of each ionic species in a mixture cannot be derived from the I-V curve. In general, measurements with single-salt feed solutions are experimentally more convenient as they do not require analyzing the composition of the permeate or receiving solution. However, it is unclear whether selectivity measured with single-salt feed solutions can in fact represent the selectivity measured with feed solutions of mixed salts. To answer this question, we evaluated cation selectivity (Mg^{2+} vs. Na^{+}) using both feed solutions with single salts and mixed salts in both pressure-driven filtration and diffusion driven by concentration difference.

Filtration In filtration, NaCl rejection was much lower with a mixed-salt feed solution compared to that with a single-salt feed solution (Fig. 5A), suggesting Donnan exclusion promotes the more permeable salt to partition more strongly into the membrane matrix.[55–57] For $MgCl_2$, the rejection

measured with a mixed-salt feed solution was also lower at a relatively low feed concentration (25 mM for each salt), whereas the difference in Mg^{2+} rejections measured using different types of feed solution diminished as the feed concentration increased. The overall ionic strength was higher in a mixed salt feed solution, which enhanced the charge screening effect and thus reduced NaCl rejection.

As discussed previously, selectivity based on solute rejections is more sensitive to the rejection of the less permeable solute and becomes highly sensitive in the range of very high (close to 100%) rejection. Thus, when the rejection of $MgCl_2$ measured with a mixed-salt feed solution increased and approached 100% as the molar concentration increased, the Na^+/Mg^{2+} selectivity also increased significantly (Fig. 5B). This trend of selectivity change with feed concentration also differed substantially from that measured using single-salt feed solutions. In fact, we cannot even conclude with confidence if selectivity is higher when measured using a single-salt feed solution or a mixed salt feed solution, as the conclusion depends on the feed concentration (Fig. 5B).

Diffusion In the diffusion experiments (with sucrose addition to offset osmosis), the measured NaCl and $MgCl_2$ diffusion fluxes were significantly lower when measured with a mixed salt feed solution (Fig. 5C). As osmosis was offset, the flux reduction compared to that measured with a single-salt feed solution is attributable to the enhanced ionic strength and thus stronger ion-ion interaction. The selectivity measured using single-salt feed solution was higher than that measured using a mixed-salt feed solution, but both remained nearly constant regardless of feed concentration (Fig. 5D). Diffusion experiments with osmosis showed similar results except that the selectivity measured in single-salt feed solution increased with concentration (Fig. S7).

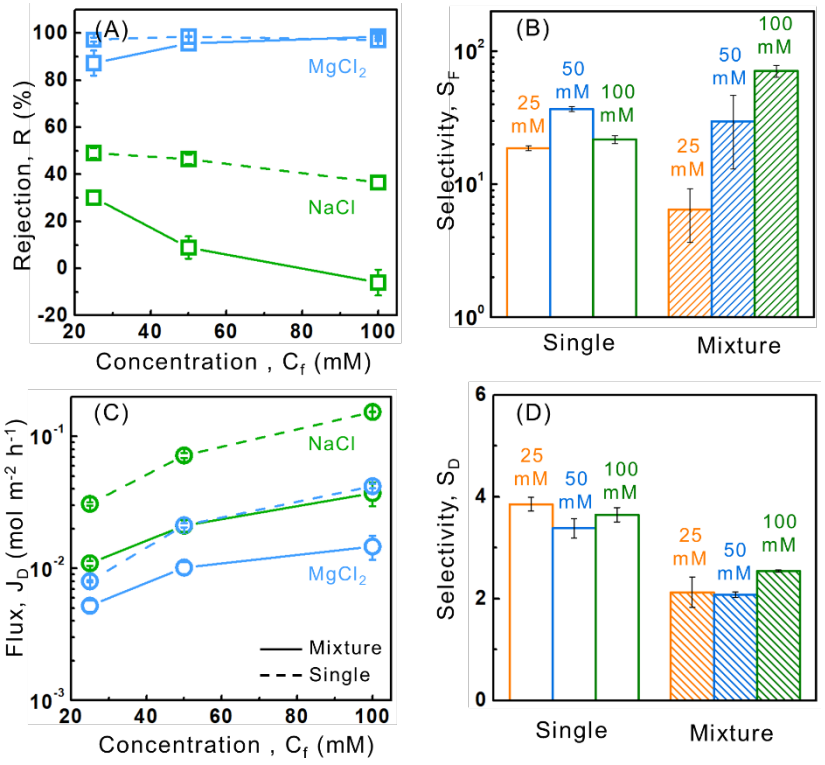

Figure 5. (A) Rejection of NaCl and $MgCl_2$ measured in single (dash) and mixture (solid) salt solutions. Filtration pressure was tuned to maintain a permeate flux of 30 L m^{-2} h^{-1} (B) Comparison of Na^+/Mg^{2+} selectivity defined on rejection in single and mixture salt solutions. (C) Diffusion flux of NaCl and $MgCl_2$ measured in single (dash) and mixture (solid) salt solutions. Osmosis was offset with sucrose solution as permeate. (D) Comparison of Na^+/Mg^{2+} selectivity defined on diffusion flux in single and mixture salt solutions. Results under three feed concentrations (i.e., 25 mM, 50 mM, 100 mM for each salt) were presented.

IMPLICATIONS AND PERSPECTIVE

The development of membranes capable of precise solute-solute separation is still in its burgeoning stage without a standardized protocol for evaluating selectivity. The results from this study unveil the inconvenient truth that selectivity measured using different methods, or even different conditions with the same method, are generally not comparable. The cross-method incomparability is true for both apparent selectivity, defined as the ratio between concentration-normalized fluxes, and the "more intrinsic" selectivity, defined as the ratio between the permeabilities of solutes through the active separation layer. The difference in selectivity measured using different methods stems from the fundamental differences in ion transport driving force, the effect of water transport, and the interaction between cation and anion transport. Further adding to the complication of selectivity measurement is the difference in selectivity measured using feed solutions containing single salt species and that containing mixed salt. While many previous studies reported selectivity based on measurements using single-salt feed solutions, those results cannot accurately represent the practically more relevant selectivity for a mixed-salt feed solution. We believe some selectivity measurements are intrinsically not comparable (e.g., results from single salt experiments vs. mixed salt experiments), whereas other selectivity measurements may eventually be relatable (e.g., results from single salt experiments in filtration vs. diffusion) but will require a more complicated theoretical framework and/or more careful experimental design to eliminate artifacts.

As most results reported in literature were inherently incomparable, we face a predicament in attempting to acquire a coherent understanding about where we are in developing advanced membranes with enhanced solute-solute selectivity. From the perspective of practical application (in nanofiltration), one should always evaluate the selectivity using pressure-driven filtration with a mixed-salt feed solution of a composition relevant to the specific applications. Here, the composition includes the concentrations of both targeted solutes and other major background solutes. For example, Li^+/Mg^{2+} selectivity in nanofiltration is likely dependent not only on the concentrations of Li^+ and Mg^{2+} but also on the ionic strength of solution. Therefore, when a membrane is developed for a specific target application, its selectivity should be evaluated under corresponding conditions and those conditions should be reported in detail.

When membranes are developed without a very specific application context, the evaluation of their solute-solute selectivity following a consistent protocol can facilitate fair performance comparison with other membranes. We propose that filtration with mixed-salt feed solutions are

preferred as the standard method for selectivity evaluation due to its strongest practical relevance. In the cases of novel membranes that cannot be scaled up or fabricated in a sufficiently robust form for pressurized filtration, the selectivity data can still be collected and should be treated with caution and should not be directly compared with data collected in filtration. Additionally, the experimental conditions should also be standardized for pressure-driven filtration including the feed composition (i.e., concentration of each salt species) and the permeate flux (which can be controlled by varying pressure). Furthermore, to ensure the statistical reliability of the reported membrane performance, we suggest not only performing replicate experiments but doing so using different samples of the same membrane.

We further encourage future studies to evaluate their membranes using pressure-driven filtration at a permeate flux of 50 L m^{-2} h^{-1} with a solution of $MgCl_2$ (25 mM) and NaCl (25 mM) for evaluating cation selectivity (Mg^{2+}/Na^{+}) and a solution of Na_2SO_4 (25 mM) and NaCl (25 mM) for evaluating anion selectivity (SO_4^{2-}/Cl^{-}). If other types of selectivity (e.g., Ca^{2+}/Na^{+}, Mg^{2+}/Li^{+}, Na^{+}/K^{+}) are of interest, they can also be evaluated at the same flux and concentrations. While we understand that these choices of flux and concentrations are arbitrary and bear no practical significance, we hope that the proposed standardization of testing conditions can provide common ground to cross-compare the performance of membranes developed in different research groups.

ASSOCIATED CONTENT

The Supporting Information is available free of charge at: XXX

Salt rejections as a function of permeate flux under different feed concentrations (Figure S1); Salt concentration in the receiving solution as a function of diffusion time under different feed concentrations (Figure S2); I-V curves with and without membranes under different feed concentrations (Figure S3); Dependence of membrane potential on the concentration ratio between the two chambers (Figure S4); Solute permeability and solute-solute selectivity as a function of concentration (Figure S5); Solute permeability and cation selectivity of different definitions in a polycarbazole-type conjugated microporous polymer membrane (Figure S6); Diffusion flux and selectivity of NaCl and $MgCl_2$ measured in single and mixture salt solutions (Figure S7).

ACKNOWLEDGEMENT

The authors S.Lin and R. Wang are thankful to the generous support from the US National Science Foundation via research grant 2017998 and from the Paul L. Busch Award from the Water Research Foundation. C. Tang acknowledges the support from the Research Grants Council of the Hong Kong Special Administration Region, China via GRF 17204220. J. Zhang appreciates the financial support from Undergraduate Research Fellowship Program at The University of Hong Kong.

REFERENCES

(1) Elimelech, M.; Phillip, W. A. The Future of Seawater Desalination: Energy, Technology, and the Environment. *Science (80-.).* **2011**, *333* (6043), 712–717. https://doi.org/10.1126/science.1200488.

(2) Epsztein, R.; DuChanois, R. M.; Ritt, C. L.; Noy, A.; Elimelech, M. Towards Single-Species Selectivity of Membranes with Subnanometre Pores. *Nat. Nanotechnol.* **2020**, *15* (6), 426–436. https://doi.org/10.1038/s41565-020-0713-6.

(3) DuChanois, R. M.; Porter, C. J.; Violet, C.; Verduzco, R.; Elimelech, M. Membrane Materials for Selective Ion Separations at the Water–Energy Nexus. *Adv. Mater.* **2021**, *2101312*, 1–18. https://doi.org/10.1002/adma.202101312.

(4) Zhao, Y.; Tong, T.; Wang, X.; Lin, S.; Reid, E. M.; Chen, Y. Differentiating Solutes with Precise Nanofiltration for Next Generation Environmental Separations: A Review. *Environ. Sci. Technol.* **2021**, *55* (3), 1359–1376. https://doi.org/10.1021/acs.est.0c04593.

(5) Lin, S.; Hatzell, M.; Liu, R.; Wells, G.; Xie, X. Mining Resources from Water. *Resour. Conserv. Recycl.* **2021**, *175* (August), 105853. https://doi.org/10.1016/j.resconrec.2021.105853.

(6) Amann, A.; Zoboli, O.; Krampe, J.; Rechberger, H.; Zessner, M.; Egle, L. Environmental Impacts of Phosphorus Recovery from Municipal Wastewater. *Resour. Conserv. Recycl.* **2018**, *130* (December 2017), 127–139. https://doi.org/10.1016/j.resconrec.2017.11.002.

(7) Tong, T.; Wallace, A. F.; Zhao, S.; Wang, Z. Mineral Scaling in Membrane Desalination: Mechanisms, Mitigation Strategies, and Feasibility of Scaling-Resistant Membranes. *J. Memb. Sci.* **2019**, *579* (February), 52–69. https://doi.org/10.1016/j.memsci.2019.02.049.

(8) Cheng, W.; Liu, C.; Tong, T.; Epsztein, R.; Sun, M.; Verduzco, R.; Ma, J.; Elimelech, M. Selective Removal of Divalent Cations by Polyelectrolyte Multilayer Nanofiltration Membrane: Role of Polyelectrolyte Charge, Ion Size, and Ionic Strength. *J. Memb. Sci.* **2018**, *559* (January), 98–106. https://doi.org/10.1016/j.memsci.2018.04.052.

(9) Li, X.; Mo, Y.; Qing, W.; Shao, S.; Tang, C. Y.; Li, J. Membrane-Based Technologies for Lithium Recovery from Water Lithium Resources: A Review. *J. Memb. Sci.* **2019**, *591* (July), 117317. https://doi.org/10.1016/j.memsci.2019.117317.

(10) Yang, G.; Shi, H.; Liu, W.; Xing, W.; Xu, N. Investigation of Mg2+/Li+ Separation by Nanofiltration. *Chinese J. Chem. Eng.* **2011**, *19* (4), 586–591. https://doi.org/10.1016/S1004-9541(11)60026-8.

(11) Wang, L.; Rehman, D.; Sun, P. F.; Deshmukh, A.; Zhang, L.; Han, Q.; Yang, Z.; Wang, Z.; Park, H. D.; Lienhard, J. H.; Tang, C. Y. Novel Positively Charged Metal-Coordinated Nanofiltration Membrane for Lithium Recovery. *ACS Appl. Mater. Interfaces* **2021**, *13* (14), 16906–16915. https://doi.org/10.1021/acsami.1c02252.

(12) Song, X.; Luo, W.; Hai, F. I.; Price, W. E.; Guo, W.; Ngo, H. H.; Nghiem, L. D. Resource Recovery from Wastewater by Anaerobic Membrane Bioreactors: Opportunities and

Challenges. *Bioresour. Technol.* **2018**, *270* (June), 669–677. https://doi.org/10.1016/j.biortech.2018.09.001.

(13) Luo, T.; Abdu, S.; Wessling, M. Selectivity of Ion Exchange Membranes: A Review. *J. Memb. Sci.* **2018**, *555* (December 2017), 429–454. https://doi.org/10.1016/j.memsci.2018.03.051.

(14) Nativ, P.; Fridman-Bishop, N.; Gendel, Y. Ion Transport and Selectivity in Thin Film Composite Membranes in Pressure-Driven and Electrochemical Processes. *J. Memb. Sci.* **2019**, *584* (October 2018), 46–55. https://doi.org/10.1016/j.memsci.2019.04.041.

(15) Liang, Y.; Zhu, Y.; Liu, C.; Lee, K. R.; Hung, W. S.; Wang, Z.; Li, Y.; Elimelech, M.; Jin, J.; Lin, S. Polyamide Nanofiltration Membrane with Highly Uniform Sub-Nanometre Pores for Sub-1 Å Precision Separation. *Nat. Commun.* **2020**, *11* (1), 1–9. https://doi.org/10.1038/s41467-020-15771-2.

(16) Liu, Y. ling; Wang, X. mao; Yang, H. wei; Xie, Y. F.; Huang, X. Preparation of Nanofiltration Membranes for High Rejection of Organic Micropollutants and Low Rejection of Divalent Cations. *J. Memb. Sci.* **2019**, *572* (September 2018), 152–160. https://doi.org/10.1016/j.memsci.2018.11.013.

(17) Boo, C.; Wang, Y.; Zucker, I.; Choo, Y.; Osuji, C. O.; Elimelech, M. High Performance Nanofiltration Membrane for Effective Removal of Perfluoroalkyl Substances at High Water Recovery. *Environ. Sci. Technol.* **2018**, *52* (13), 7279–7288. https://doi.org/10.1021/acs.est.8b01040.

(18) Lu, Y.; Wang, R.; Zhu, Y.; Wang, Z.; Fang, W.; Lin, S.; Jin, J. Two-Dimensional Fractal Nanocrystals Templating for Substantial Performance Enhancement of Polyamide Nanofiltration Membrane. *Proc. Natl. Acad. Sci. U. S. A.* **2021**, 1–7. https://doi.org/10.1073/pnas.2019891118/-/DCSupplemental.Published.

(19) Gao, S.; Zhu, Y.; Gong, Y.; Wang, Z.; Fang, W.; Jin, J. Ultrathin Polyamide Nanofiltration Membrane Fabricated on Brush-Painted Single-Walled Carbon Nanotube Network Support for Ion Sieving. *ACS Nano* **2019**, *13* (5), 5278–5290. https://doi.org/10.1021/acsnano.8b09761.

(20) Liu, T. Y.; Yuan, H. G.; Li, Q.; Tang, Y. H.; Zhang, Q.; Qian, W.; Bruggen, B. Van Der; Wang, X. Ion-Responsive Channels of Zwitterion-Carbon Nanotube Membrane for Rapid Water Permeation and Ultrahigh Mono-/Multivalent Ion Selectivity. *ACS Nano* **2015**, *9* (7), 7488–7496. https://doi.org/10.1021/acsnano.5b02598.

(21) Zhang, H. Z.; Xu, Z. L.; Ding, H.; Tang, Y. J. Positively Charged Capillary Nanofiltration Membrane with High Rejection for Mg2 + and Ca2 + and Good Separation for Mg2 + and Li +. *Desalination* **2017**, *420* (May), 158–166. https://doi.org/10.1016/j.desal.2017.07.011.

(22) Al-Hamadani, Y. A. J.; Jun, B. M.; Yoon, M.; Taheri-Qazvini, N.; Snyder, S. A.; Jang, M.; Heo, J.; Yoon, Y. Applications of MXene-Based Membranes in Water Purification: A Review. *Chemosphere* **2020**, *254*, 126821. https://doi.org/10.1016/j.chemosphere.2020.126821.

(23) Hirunpinyopas, W.; Prestat, E.; Worrall, S. D.; Haigh, S. J.; Dryfe, R. A. W.; Bissett, M. A. Desalination and Nanofiltration through Functionalized Laminar MoS2 Membranes. *ACS Nano* **2017**, *11* (11), 11082–11090. https://doi.org/10.1021/acsnano.7b05124.

(24) Hu, R.; He, Y.; Zhang, C.; Zhang, R.; Li, J.; Zhu, H. Graphene Oxide-Embedded Polyamide Nanofiltration Membranes for Selective Ion Separation. *J. Mater. Chem. A* **2017**, *5* (48), 25632–25640. https://doi.org/10.1039/c7ta08635k.

(25) Zhang, H.; Hou, J.; Hu, Y.; Wang, P.; Ou, R.; Jiang, L.; Zhe Liu, J.; Freeman, B. D.; Hill, A. J.; Wang, H. Ultrafast Selective Transport of Alkali Metal Ions in Metal Organic Frameworks with Subnanometer Pores. *Sci. Adv.* **2018**, *4* (2). https://doi.org/10.1126/sciadv.aaq0066.

(26) Yuan, S.; Li, X.; Zhu, J.; Zhang, G.; Van Puyvelde, P.; Van Der Bruggen, B. Covalent Organic Frameworks for Membrane Separation. *Chem. Soc. Rev.* **2019**, *48* (10), 2665–2681. https://doi.org/10.1039/c8cs00919h.

(27) He, Z.; Zhou, J.; Lu, X.; Corry, B. Bioinspired Graphene Nanopores with Voltage-Tunable Ion Selectivity for Na+ and K+. *ACS Nano* **2013**, *7* (11), 10148–10157. https://doi.org/10.1021/nn4043628.

(28) Werber, J. R.; Porter, C. J.; Elimelech, M. A Path to Ultraselectivity: Support Layer Properties to Maximize Performance of Biomimetic Desalination Membranes. *Environ. Sci. Technol.* **2018**, *52* (18), 10737–10747. https://doi.org/10.1021/acs.est.8b03426.

(29) Geise, G. M. Experimental Characterization of Polymeric Membranes for Selective Ion Transport. *Curr. Opin. Chem. Eng.* **2020**, *28*, 36–42. https://doi.org/10.1016/j.coche.2020.01.002.

(30) Zhou, Z.; Guo, D.; Shinde, D. B.; Cao, L.; Li, Z.; Li, X.; Lu, D.; Lai, Z. Precise Sub-Angstrom Ion Separation Using Conjugated Microporous Polymer Membranes. *ACS Nano* **2021**, *15* (7), 11970–11980. https://doi.org/10.1021/acsnano.1c03194.

(31) Abraham, J.; Vasu, K. S.; Williams, C. D.; Gopinadhan, K.; Su, Y.; Cherian, C. T.; Dix, J.; Prestat, E.; Haigh, S. J.; Grigorieva, I. V.; Carbone, P.; Geim, A. K.; Nair, R. R. Tunable Sieving of Ions Using Graphene Oxide Membranes. *Nat. Nanotechnol.* **2017**, *12* (6), 546–550. https://doi.org/10.1038/nnano.2017.21.

(32) Ren, C. E.; Hatzell, K. B.; Alhabeb, M.; Ling, Z.; Mahmoud, K. A.; Gogotsi, Y. Charge-and Size-Selective Ion Sieving Through Ti3C2Tx MXene Membranes. *J. Phys. Chem. Lett.* **2015**, *6* (20), 4026–4031. https://doi.org/10.1021/acs.jpclett.5b01895.

(33) Zhang, C.; Mu, Y.; Zhang, W.; Zhao, S.; Wang, Y. PVC-Based Hybrid Membranes Containing Metal-Organic Frameworks for Li+/Mg2+ Separation. *J. Memb. Sci.* **2020**, *596* (November 2019), 117724. https://doi.org/10.1016/j.memsci.2019.117724.

(34) Yao, Z.; Guo, H.; Yang, Z.; Qing, W.; Tang, C. Y. Preparation of Nanocavity-Contained Thin Film Composite Nanofiltration Membranes with Enhanced Permeability and Divalent to Monovalent Ion Selectivity. *Desalination* **2018**, *445* (May), 115–122. https://doi.org/10.1016/j.desal.2018.07.023.

(35) Li, S. L.; Shan, X.; Zhao, Y.; Hu, Y. Fabrication of a Novel Nanofiltration Membrane

with Enhanced Performance via Interfacial Polymerization through the Incorporation of a New Zwitterionic Diamine Monomer. *ACS Appl. Mater. Interfaces* **2019**, *11* (45), 42846–42855. https://doi.org/10.1021/acsami.9b15811.

(36) Xu, P.; Wang, W.; Qian, X.; Wang, H.; Guo, C.; Li, N.; Xu, Z.; Teng, K.; Wang, Z. Positive Charged PEI-TMC Composite Nanofiltration Membrane for Separation of Li+ and Mg2+ from Brine with High Mg2+/Li+ Ratio. *Desalination* **2019**, *449* (October 2018), 57–68. https://doi.org/10.1016/j.desal.2018.10.019.

(37) Guo, Y.; Ying, Y.; Mao, Y.; Peng, X.; Chen, B. Polystyrene Sulfonate Threaded through a Metal–Organic Framework Membrane for Fast and Selective Lithium-Ion Separation. *Angew. Chemie - Int. Ed.* **2016**, *55* (48), 15120–15124. https://doi.org/10.1002/anie.201607329.

(38) Wen, Q.; Yan, D.; Liu, F.; Wang, M.; Ling, Y.; Wang, P.; Kluth, P.; Schauries, D.; Trautmann, C.; Apel, P.; Guo, W.; Xiao, G.; Liu, J.; Xue, J.; Wang, Y. Highly Selective Ionic Transport through Subnanometer Pores in Polymer Films. *Adv. Funct. Mater.* **2016**, *26* (32), 5796–5803. https://doi.org/10.1002/adfm.201601689.

(39) Zhou, X.; Wang, Z.; Epsztein, R.; Zhan, C.; Li, W.; Fortner, J. D.; Pham, T. A.; Kim, J. H.; Elimelech, M. Intrapore Energy Barriers Govern Ion Transport and Selectivity of Desalination Membranes. *Sci. Adv.* **2020**, *6* (48), 1–10. https://doi.org/10.1126/sciadv.abd9045.

(40) Strathmann, H. *Ion-Exchange Membrane Separation Processes*, 1st ed.; Elsevier Science, 2004.

(41) Wang, R.; Lin, S. Pore Model for Nanofiltration: History, Theoretical Framework, Key Predictions, Limitations, and Prospects. *J. Memb. Sci.* **2021**, *620* (October 2020), 118809. https://doi.org/10.1016/j.memsci.2020.118809.

(42) Luo, J.; Wan, Y. Effects of PH and Salt on Nanofiltration-a Critical Review. *J. Memb. Sci.* **2013**, *438*, 18–28. https://doi.org/10.1016/j.memsci.2013.03.029.

(43) Nghiem, L. D.; Schäfer, A. I.; Elimelech, M. Role of Electrostatic Interactions in the Retention of Pharmaceutically Active Contaminants by a Loose Nanofiltration Membrane. *J. Memb. Sci.* **2006**, *286* (1–2), 52–59. https://doi.org/10.1016/j.memsci.2006.09.011.

(44) Deen, W. M. Hindered Transport of Large Molecules in Liquid-filled Pores. *AIChE J.* **1987**, *33* (9), 1409–1425. https://doi.org/10.1002/aic.690330902.

(45) Wang, D. X.; Su, M.; Yu, Z. Y.; Wang, X. L.; Ando, M.; Shintani, T. Separation Performance of a Nanofiltration Membrane Influenced by Species and Concentration of Ions. *Desalination* **2005**, *175* (2), 219–225. https://doi.org/10.1016/j.desal.2004.10.009.

(46) Peeters, J. M. M., Boom, J. P., Mulder, M. H. V., & Strathmann, H. (1998). Retention Measurements of Nanofiltration Membranes with Electrolyte Solutions. Journal of Membrane Science 145(2). **1998**, *145*, 199-209.

(47) Marcus, Y. A Simple Empirical Model Describing the Thermodynamics of Hydration of Ions of Widely Varying Charges, Sizes, and Shapes. *Biophys. Chem.* **1994**, *51* (2–3), 111–127. https://doi.org/10.1016/0301-4622(94)00051-4.

(48) Jin, X.; She, Q.; Ang, X.; Tang, C. Y. Removal of Boron and Arsenic by Forward Osmosis Membrane: Influence of Membrane Orientation and Organic Fouling. *J. Memb. Sci.* **2012**, *389*, 182–187. https://doi.org/10.1016/j.memsci.2011.10.028.

(49) Yang, Z.; Guo, H.; Tang, C. Y. The Upper Bound of Thin-Film Composite (TFC) Polyamide Membranes for Desalination. *J. Memb. Sci.* **2019**, *590* (June), 117297. https://doi.org/10.1016/j.memsci.2019.117297.

(50) Wijmans, J. G.; Baker, R. W. The Solution-Diffusion Model : A Review. **1995**, *107*, 1–21.

(51) Gao, Y.; Wang, Y. N.; Li, W.; Tang, C. Y. Characterization of Internal and External Concentration Polarizations during Forward Osmosis Processes. *Desalination* **2014**, *338* (1), 65–73. https://doi.org/10.1016/j.desal.2014.01.021.

(52) Mulder, M. *Basic Principles of Membrane Technology*, Second.; Springer Science & Business Media, 2012.

(53) Tang, C.; Yaroshchuk, A.; Bruening, M. L. Flow through Negatively Charged, Nanoporous Membranes Separates Li+and K+due to Induced Electromigration. *Chem. Commun.* **2020**, *56* (74), 10954–10957. https://doi.org/10.1039/d0cc03143g.

(54) Tedesco, M.; Hamelers, H. V. M.; Biesheuvel, P. M. Nernst-Planck Transport Theory for (Reverse) Electrodialysis: II. Effect of Water Transport through Ion-Exchange Membranes. *J. Memb. Sci.* **2017**, *531* (September 2016), 172–182. https://doi.org/10.1016/j.memsci.2017.02.031.

(55) Yaroshchuk, A. E. Negative Rejection of Ions in Pressure-Driven Membrane Processes. *Adv. Colloid Interface Sci.* **2008**, *139* (1–2), 150–173. https://doi.org/10.1016/j.cis.2008.01.004.

(56) Yaroshchuk, A.; Bruening, M. L. An Analytical Solution of the Solution-Diffusion-Electromigration Equations Reproduces Trends in Ion Rejections during Nanofiltration of Mixed Electrolytes. *J. Memb. Sci.* **2017**, *523* (September 2016), 361–372. https://doi.org/10.1016/j.memsci.2016.09.046.

(57) Yaroshchuk, A.; Bruening, M. L.; Zholkovskiy, E. Modelling Nanofiltration of Electrolyte Solutions. *Adv. Colloid Interface Sci.* **2019**, *268*, 39–63. https://doi.org/10.1016/j.cis.2019.03.004.

Table of Contents Graphic

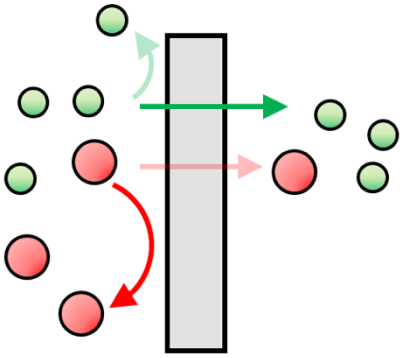

*Can we compare **solute-solute selectivity** measured in different studies?*

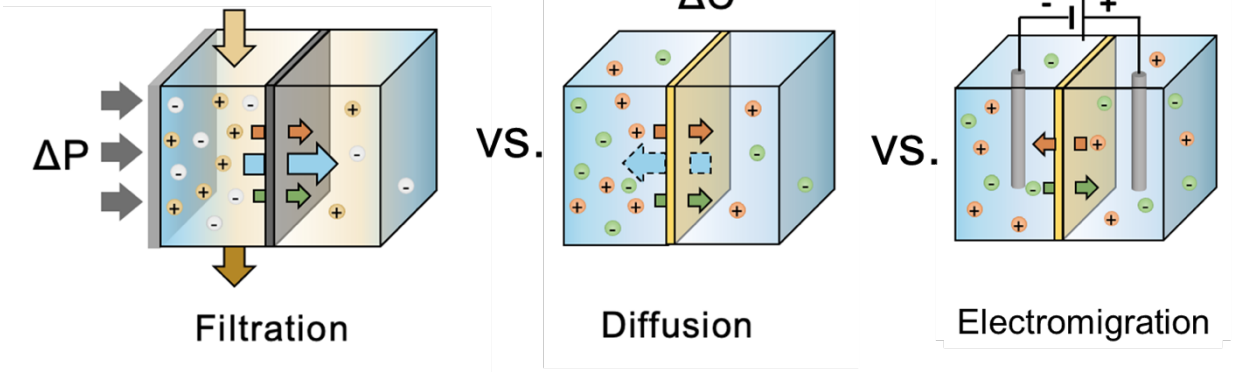

833